NEUTRON REFLECTOMETRY

A.A. van Well
IRI, Delft

1. INTRODUCTION

On July 14, 1944, Fermi discovered that neutrons could be totally reflected from a surface [1]. The recognition that this was a direct consequence of the wave character of the neutron resulted in the assessment of many analogies between neutrons and light. This part of Neutron research where reflection, refraction, and interference play an essential role is generally referred to as 'neutron optics'. Klein and Werner [2, 3] give an extensive review of many aspects of neutron optics. For a very good and clear introduction in this field, we refer to Sears [4]. Analogous to optics with visible light, a refractive index n for neutron can be defined for each material. If we define n = 1 in vacuum, it appears that for almost all materials the refractive index for thermal neutrons is smaller than unity. The deviations from 1 are in the order of 10^{-5}. This implies that for most materials total reflection will occur at small glancing angles (of the of a fraction of 1 degree) coming from the vacuum (or air), just opposite the normal situation for light. The neutron wavelength, the scattering length density and the magnetic properties of the material determine the critical angle for total reflection. We will come back to this in detail in the next sections. Total reflection of neutrons is extensively applied in the determination of the neutron scattering length [5], for the transport of neutrons over long distances (10 - 100 m) in neutron guides [6], in filter systems [7], and neutron polarisers [8-10]. In the latter application, use is made of the fact that the interaction of neutrons with spin parallel to the magnetic induction differs from that with the anti-parallel spin.

So in the early stages, the phenomenon of total reflection was used to construct instrument components. Much later one realised that detailed information about surface and interface structure could be obtained by determining the (partially) reflected neutron intensity 'beyond' the total reflection region. This information concerns the composition as well as magnetic profiles as a function of z, the distance tot the interface. The spatial range extends from a fraction of 1 nm (monolayers) to depths of a few hundred nanometres. This insight resulted in a fast growing number of neutron reflectometers all over the world, with a still broadening range of applications.

Generally, samples are being studied that are isotropic in the x-y plane, parallel to the interface. This means perfectly layered structures along an area of the order of several cm^2. For these systems, the neutron reflects purely specularly (angle of incidence = angle of reflection). In principle, information about lateral structure (in the range from 100 nm to several μm) could be obtained from the intensity distribution of the non-specularly reflected neutrons. This is a new and complex branch of neutron reflection that is still maturing [11, 12] and will not be considered here.

Neutron reflectometry and the reflection of electro-magnetic waves with the E-vector perpendicular to the plane of reflection, the so-called s-waves, are described by the same equation. Lekner [13] extensively reviews the theoretical background and gives exact and approximate solution methods for both EM-waves and particles. In Section 2, the theoretical background will be discussed briefly. The phenomenon of reflection is described by the Schrödinger equation, where the medium is considered to be continuous and is characterised by means of an effective (or 'optical') potential. This potential can be translated into an

The theoretical background of neutron reflection, experimental methods and the interpretation of reflection data are presented.

expression for the refractive index. In Section 3, some words are spent on the interpretation of neutron reflection data. For a recent review of this field, we advice [14]. Section 4 discusses the experimental methods. In Section 5, we conclude with some examples of the application of neutron reflectometry.

2. THEORETICAL BACKGROUND

The neutron is described by a plane wave with wave vector **k**, with magnitude $k = 2\pi/\lambda$, and with kinetic energy

$$E = \frac{\hbar^2 k^2}{2m}. \tag{1}$$

The interaction with matter is described by an effective or 'optical' potential [4]

$$V(\mathbf{r}) = \frac{2\pi\hbar^2}{m}\rho(\mathbf{r}) - \boldsymbol{\mu}_n \cdot \mathbf{B}(\mathbf{r}), \tag{2}$$

where the first term describes the interaction with the nuclei and the second term the magnetic interaction, m is the neutron mass, μ_n the neutron magnetic moment, **B** the magnetic induction (throughout this paper we use SI units), and the scattering length density is defined by

$$\rho(\mathbf{r}) = <\sum_i N_i b_i>, \tag{3}$$

where N_i and b_i are the number density and coherent scattering length of species i, and <···> denotes the average at position **r**. Neutron absorption is taken into account by the imaginary part of the scattering length b [4]

$$b = b' - ib'', \tag{4}$$

where $b'' = (k/4\pi)\sigma_a(k)$, with σ_a the absorption cross section. Except for thick layers and/or strongly absorbing elements, such as Cd and Gd, the adsorption can in general be neglected.

Reflection is governed by the 3-dimensinal Schrödinger equation

$$-\frac{\hbar^2}{2m}\nabla^2\Psi(\mathbf{r}) + V(\mathbf{r})\Psi(\mathbf{r}) = E(\mathbf{k})\Psi(\mathbf{r}). \tag{5}$$

If we consider a system that is isotropic in the x, y plane, then the potential V only depends on the perpendicular component z (see Fig. 1). Eq. (5) then reduces to the 1-dimensional equation

$$\frac{\mathrm{d}^2\psi(z)}{\mathrm{d}z^2} + \left(q_0^2 - \Gamma(z)\right)\psi(z) = 0, \tag{6}$$

with $\psi(z)$ the perpendicular component of the neutron wave function, and $q_0 = k_0 \sin\theta_0$ is the perpendicular component of the neutron wave vector in the incoming medium ($z < 0$). Note that the wave vector transfer during reflection is given by $Q = 2q_0$. The optical potential in units of wave vector squared is defined by

$$\Gamma(z) = \frac{2m}{\hbar^2}V(z). \tag{7}$$

The perpendicular component of the neutron wave vector as a function of depth is

$$q(z) = \sqrt{q_0 - \Gamma(z)}. \tag{8}$$

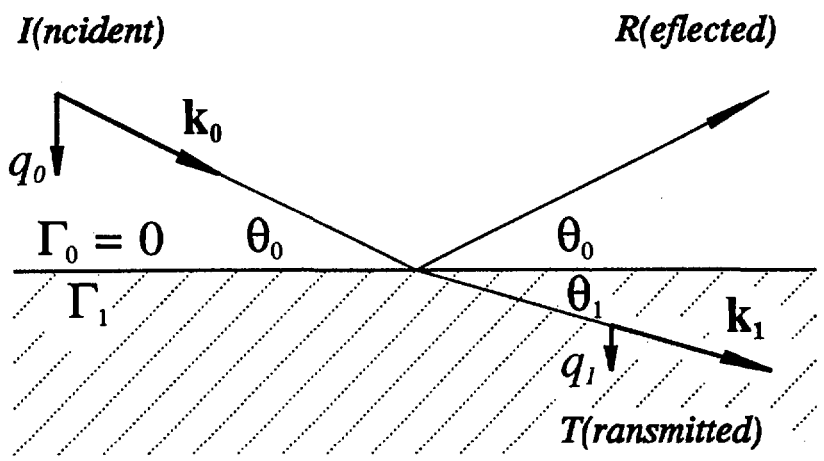

Fig. 1. Reflection geometry

In Eq. (6), the incoming medium was taken vacuum (or air) with $\Gamma = 0$. If the neutron approaches the interface through a bulk medium with $\Gamma = \Gamma_0$, $\Gamma(z)$ should be replaced by $\Gamma(z)$-Γ_0. The nuclear part of $\Gamma(z)$ is given by

$$\Gamma_n(z) = 4\pi\rho(z) = 4\pi < \sum_i N_i b_i > . \tag{9}$$

The treatment of the magnetic part is more complicated. Here we will only consider the collinear case, i.e. where the neutron spin is either parallel or anti-parallel to the magnetic induction **B**. Then the magnetic part of Γ can be written as

$$\Gamma_m(z) = \pm 4\pi < \sum_i N_i p_i >, \tag{10}$$

resulting in

$$\Gamma(z) = \Gamma_n(z) + \Gamma_m(z) = 4\pi < \sum_i N_i (b_i \pm p_i) >, \tag{11}$$

where the 'magnetic scattering length' is defined as

$$p_i = C\mu_i, \tag{12}$$

with μ_i the magnetic moment of species i in units of Bohr magneton μ_B and the constant given by $C = m\mu_n\mu_B\mu_0/2\pi\hbar^2 = 2.699$ fm/μ_B. The plus (minus) sign in Eqs. (10-11) refers to spin parallel (anti parallel) to the magnetic induction (or magnetisation). In the non-collinear case, the theoretical description is much more complicated [15-17]. Then, spin flip may occur during reflection, also leading to non-specular reflection [17-20].

From Eqs. (6) and (8) follows that for neutron, analogous to light, a refractive index can be defined by

$$n(z) = \frac{k(z)}{k_0} = \sqrt{1 - \frac{V(z)}{E_0}} = \sqrt{1 - \frac{\Gamma(z)}{k_0^2}}. \tag{13}$$

For the non-magnetic case this yields

$$n(z) = \sqrt{1 - \frac{\lambda^2\rho(z)}{\pi}} \approx 1 - \frac{\lambda^2\rho(z)}{2\pi}. \tag{14}$$

A sharp interface between two bulk media with $\Gamma_0 < \Gamma_1$ (see Fig.1) acts as a potential barrier for de neutron with a height $\Delta V = \hbar^2\Delta\Gamma/(2m)$, with $\Delta\Gamma = \Gamma_1 - \Gamma_0$. If the 'perpendicular component' of the kinetic energy is smaller than this barrier, total reflection occurs. I.e., the

reflected intensity $R(q_0) = 1$ for $q_0 < q_c = \sqrt{\Delta\Gamma}$. In that case, q_1 is imaginary, corresponding with an exponentially damped wave, the 'evanescent wave'. For $q_0 > q_c$ the reflectivity decays according to the Fresnel law (see dotted line in Fig. 2)

$$R_F(q_0) = \left|\frac{q_0 - q_1}{q_0 + q_1}\right|^2 \tag{15}$$

For $q_0 >> q_c$ the Fresnel reflectivity approaches the asymptotic form

$$R_F(q_0) \approx \left(\frac{q_c}{2q_0}\right)^4 = \frac{(\Delta\Gamma)^2}{16q_0^4}. \tag{16}$$

At the interface between two media with refractive indices n_0 and n_1 (conform Eq. (13)), the Snellius law holds

$$n_0 \cos\theta_0 = n_1 \cos\theta_1. \tag{17}$$

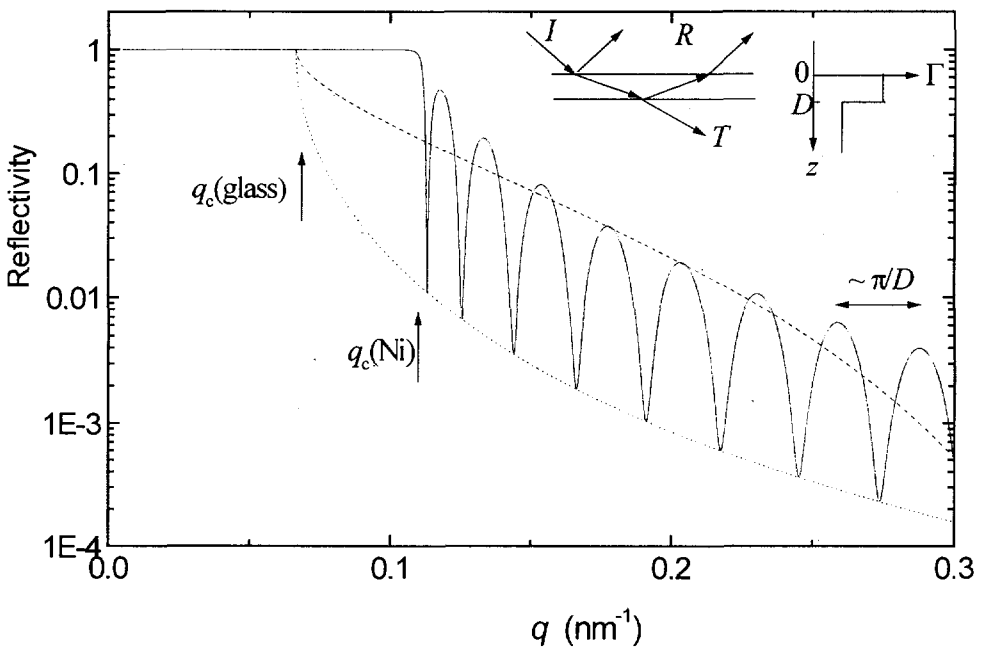

Figure 2. Calculated reflectivity from a glass substrate with a nickel layer of thickness D. Continuous line: D = 100 nm; dashed line: D = 10 nm; dotted line: bare substrate.

In our example $n_0 < n_1$ and therefore $\theta_1 < \theta_0$. For neutrons with wavelength $\lambda = 2\pi/k_0$ total reflection occurs for glancing angles smaller than the critical angle $\theta_c = \arccos(n_1/n_0) = q_c/k_0 = \sqrt{\Delta\Gamma}/k_0 = \lambda\sqrt{\Delta\Gamma}/2\pi$. For most materials the deviation of n from 1 is of the order 10^{-5}, resulting in very small critical angles, of the order 10 mrad (17.5 mrad corresponds to 1°). In Table I, numerical values for the variables discussed above are given for some materials. In Fig. 3, Γ_n (and the corresponding n) is displayed for all elements. Note that different isotope in general have different scattering lengths.

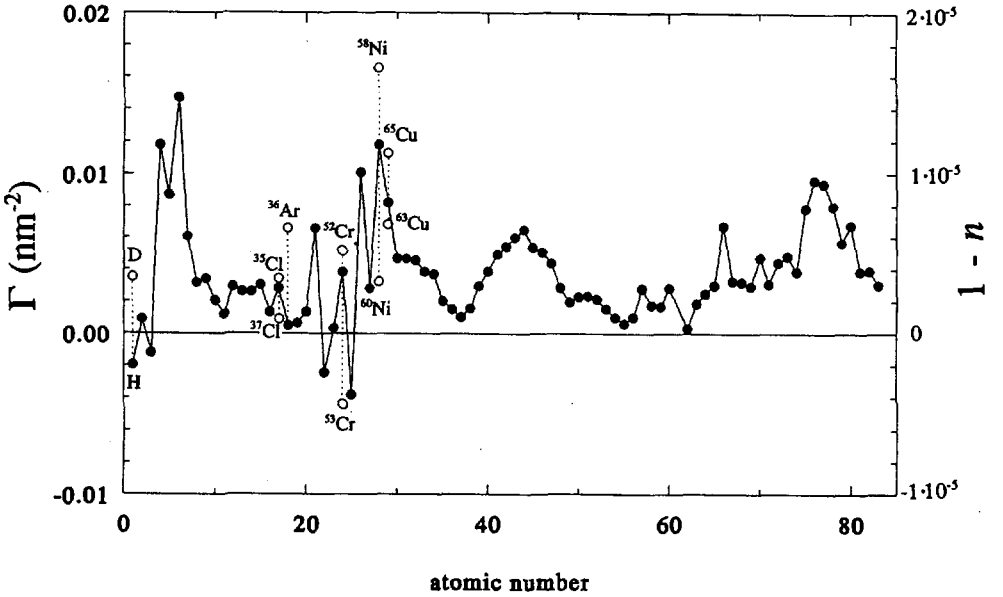

Figure 3: Γ, defined by Eq. (11), and the deviation of the refractive index from unity (for λ = 0.28 nm) as a function of the atomic number. For some elements, values for different isotopes are given. Closed circles represent natural isotopic abundance.

Table I. Neutron reflection parameters for some materials. The symbols for the magnetic materials indicate that the magnetic moment (in saturation) is not taken into account (⊙), is parallel (⊕), or anti-parallel (⊖) to the neutron spin.

material		b' (fm)	b'' (fm)	p (fm)	N (nm^{-3})	Γ (nm^{-2})	q_c (nm^{-1})	θ_c (mrad/nm)
Si	crystal	4.15	0.0	0.0	49.9	0.00260	0.0510	8.12
SiO_2	'glass'	15.75	0.0	0.0	22.0	0.00435	0.0660	10.50
Ni	⊙	10.3	0.0	0.0	91.3	0.0118	0.109	17.3
	⊕	10.3	0.0	2.0	91.3	0.0141	0.119	18.9
	⊖	10.3	0.0	-2.0	91.3	0.0095	0.0975	15.5
^{58}Ni	⊙	14.4	0.0	0.0	91.3	0.0165	0.128	20.4
	⊕	14.4	0.0	2.0	91.3	0.0188	0.137	21.8
	⊖	14.4	0.0	-2.0	91.3	0.0142	0.119	19.0
C	diamond	6.65	0.0	0.0	176.0	0.0147	0.121	19.3
C	graphite	6.65	0.0	0.0	112.8	0.0094	0.097	15.4
Al		3.45	0.0	0.0	60.3	0.00264	0.0514	8.18
Au		7.63	0.027	0.0	59.0	0.00566	0.0752	12.0
Cd		4.87	0.70	0.0	46.4	$0.00284 - 0.0005i$	0.0533	8.48
Gd		6.5	13.8	0.0	30.2	$0.00247 - 0.0035i$	0.0497	7.91
Ti		-3.43	0.0	0.0	56.6	-0.00245	0.0	0.0
Fe	⊙	9.65	0.0	0.0	84.8	0.0102	0.101	16.1
	⊕	9.65	0.0	5.8	84.8	0.0163	0.128	20.3
	⊖	9.65	0.0	-5.8	84.8	0.0040	0.063	10.1
Co	⊙	2.53	0.0	0.0	89.7	0.00281	0.053	8.44
	⊕	2.53	0.0	4.5	89.7	0.0077	0.088	14.0
	⊖	2.53	0.0	-4.5	89.7	-0.0022	0.0	0.0
H_2O		-1.677	0.0	0.0	33.4	-0.00070	0.0	0.0
D_2O		19.15	0.0	0.0	33.3	0.00800	0.0894	14.2

As a second example, we consider a substrate coated with a single layer. In this case also, an analytic expression exists [13]. The partially reflected waves from both interfaces interfere.

The positions of the interference fringes (the so-called Kiessig fringes [21]) are determined by the layer thickness, while the amplitude depends on the contrast in Γ for the three media. For $q_0 >> q_c$ the period of the oscillations approaches π/D, with D the layer thickness. In Fig. 2, the reflected intensity from a glass substrate with a nickel layer is shown. In this case the optical potential of the layer is higher than that of the substrate. For $q_0 < q_c(\mathrm{Ni})$, the 'perpendicular component' of E is smaller than the potential V of nickel. The neutron wave tunnels through the layer and is reflected / transmitted at the second interface. For a layer thickness D = 100 nm, almost total reflection occurs in the range $q_c(\mathrm{glass}) < q_0 < q_c(\mathrm{Ni})$. For a thickness D = 10 nm, the penetration depth in this q_0-region is large enough to see the influence of the buried interface.

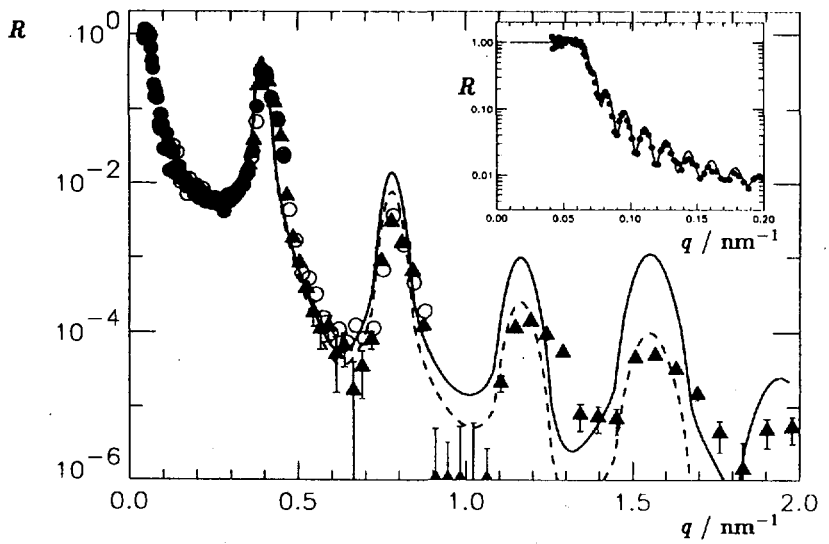

Figure 4. Reflectivity from a Ni/TiH$_x$ multilayer on silicon, consisting of 20 bilayers with 5 / 3.1 nm thicknesses. Experimental results are obtained with the time-of-flight reflectometer ROG of IRI [22], for glancing angles 7.5 (closed circles), 20.5 (open circles), and 60.4 mrad (triangles). The continuous line represents a model calculation with perfect interfaces. For the dashed line, an interfacial roughness of 0.5 nm was included.

As a third example, we consider a multilayer system composed of a stack of identical bilayers. Again, at small q_0, we recognize the Kiessig fringes, resulting from the total layer thickness. Due to the repetition of the bilayers (with bilayer thickness $d = d_{\mathrm{Ni}} + d_{\mathrm{TiH}}$) Bragg reflections are present. At large q_0 values, the peak position of the lth order Bragg peak can be approximated by $l\pi/d$.

3. INTERPRETATION

The aim of a neutron-reflection experiment is to obtain information about $\Gamma(z)$ from a measured reflection profile $R(q)$ (for sake of simplicity we omit the subscript '0' in the remainder of this paper). Usually, this is done by model fitting. Then, a model for $\Gamma(z)$, containing adjustable parameters, is used. Some kind of (weighted) least-squares routines is used, to deduce these parameters from the experimental data. The weight factors are determined by the statistical accuracy of the data. In the model calculations, the finite exprimental q-resolution is taken into account. For a continuously varying $\Gamma(z)$, it is –in general- not possible to derive an analytical expression for $R(q)$. By dividing the layer into an number of layers, each with constant Γ, the reflection profile $R(q)$ can be calculated numerically, using an optical matrix method [13, 23]. For each layer, a matrix is constructed from the boundary conditions that at the interface both $\psi(z)$ and $\mathrm{d}\psi(z)/\mathrm{d}z$ are continuous.

From the product of the matrices of the individual layers, $R(q)$ can be calculated. In this way, $R(q)$ can be calculated for all $\Gamma(z)$ to any desired accuracy. Although, due to lack of phase information, no unique solution can be obtained, this fitting procedure often leads to good results. If it appears to be difficult to find a good set of starting values for the parameters, leading to acceptable fits, other methods are available. In this case 'maximum entropy methods' [24-25] or 'genetic algorithms' [26] can be used to globally scan the parameter space. Recently, methods are being developed to obtain phase information via a specially designed set of experiments [27-31]. With this phase information it is –in principle- possible to uniquely invert the data to $\Gamma(z)$.

Besides these 'exact' methods to calculate $R(q)$, approximate methods exist [13]. The so-called kinematic approximation yields the best physical insight. This is a weak-interaction approximation, and is only valid for low reflectivities, i.e. for $q >> q_c$. It results in the following expression

$$R(q) \approx \frac{\Gamma_{\text{substrate}}}{16q^4}\left|\int_{-\infty}^{\infty}\frac{d\Gamma}{dz}\exp(i2qz)dz\right|^2, \qquad (17)$$

where the reflectivity is expressed in terms of the Fourier transform of the gradient of the density profile. The failure of Eq. (17) for some systems, even at low reflectivities, is explicitly demonstrated by Lekner [32]. Crowley [33] developed a more advanced 'kinematic' approximation, also applicable for higher values of R, i.e. smaller q values.

4. EXPERIMENTAL TECHNIQUES

Reflectivities have to be determined as a function of $q = (2\pi/\lambda) \sin\theta$. This can be realized by using a monochromatic beam, performing θ-2θ scans. This (MONO) method is often used at continuous sources. Examples: NIST (USA), KFA, HMI, GKSS (Germany), Risø (Denmark). If a broad wavelength spectrum is available, the glancing angle θ can be kept fixed, while λ is determined by means of the time-of-flight (TOF) technique. This method is the obvious choice at pulsed sources. Examples: ISIS (UK), Los Alamos (USA). The advantage of the latter method is that a large q region can be covered, without changing the geometry. De Haan *et al.* [34] made a comparison between both methods, for an instrument placed at a continuous source. If a special type of chopper is used [35], the performance of both techniques is similar. At the Delft reflectometer ROG, the TOF technique is used. In the reflectometers, presently being built at PSI and ILL, both the TOF and MONO option will be possible. Extra options, available at several reflectometers, are polarisers, spin flippers, spin analyser (all needed for properly measuring magnetic structures), and a position sensitive detector (for measuring non-specular reflection).

5. APPLICATIONS

The field of application is very broad. To give an overview, we refer to [23, 36], with references therein. Almost full account of all reflectometry research is given in the proceedings of the *Surface X-Ray and Neutron Scattering* (SXNS) conference series [37]. Here, we restrict ourselves by remarking that neutron reflectometry yields unique information is those fields where contrast variation, by means of isotope substitution, can be applied, and in the field of surface magnetism. We will demonstrate both areas with an example.

As a first example, we show the results of Lee *et al.* [38], concerning the adsorption of the surfactant decyl-trimethylammoniumbromide (DTAB, $C_{10}H_{21}N(CH_3)_3^+Br^-$) at the air/water interface.

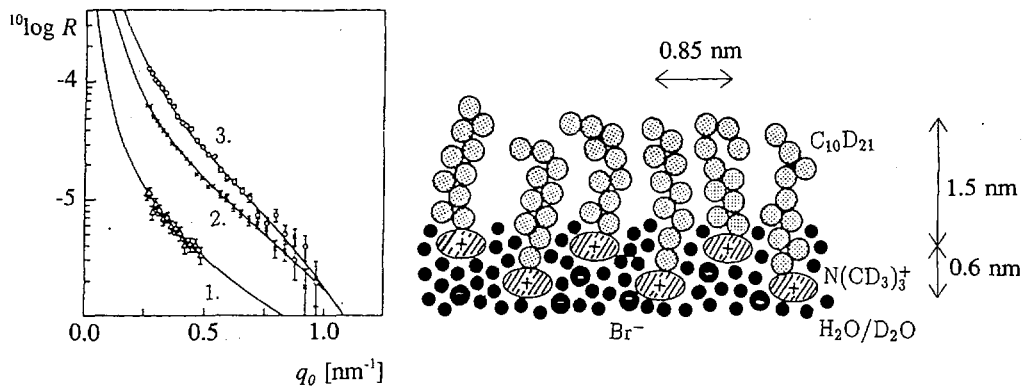

Figure 5. Left: experimental reflectivities from the air-water interface of a 0.05M solution of DTAB; 1: $C_{10}H_{21}N(CH_3)_3{}^+Br^-$; 2: $C_{10}D_{21}N(CH_3)_3{}^+Br^-$; 3: $C_{10}D_{21}N(CD_3)_3{}^+Br$.
Right: An artist impression of the structure of the adsorbed layer, obtained by simultaneously fitting the 3 data sets.

The tail of this molecule is hydrofobic and the head hydrophylic. The experiment have been performed with so-called air-contrast-matched water (a H_2O/D_2O mixture containing 8.08 vol% D_2O, yielding $\Gamma = 0$). Then all signals measured are originating from the adsorbed layer. Three different levels of deuteration of the molecule were used, yielding detailed information about the different parts of the molecule. The measured reflectivity curves with the resulting structure is shown in Fig. 5.

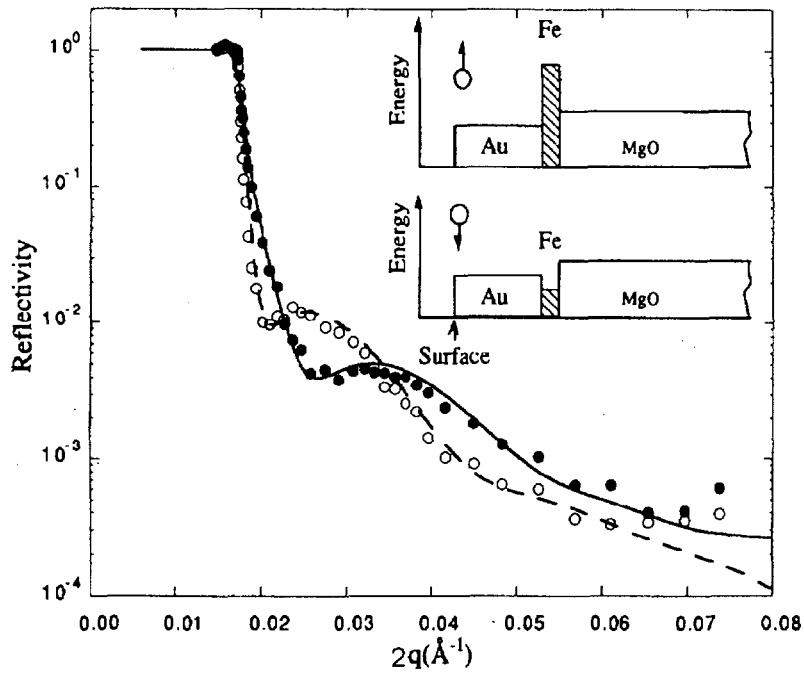

Figure 6. Reflectivity as a function of wave vector transfer 2q, of spin parallel (open circles) and spin anti-parallel (closed circles) for 1.6 nm Fe on a MgO substrate, covered with Au, in a magnetic field of 2000 Oe.

As an example of polarised neutron reflectometry, we discuss the experiment of Huang *et al.* [39] of a thin bcc iron film on MgO, covered with a gold layer. Experiments were performed

for different thicknesses of the iron layer (0.4, 0.6, 0.8, and 1.0 nm). From the data was concluded that the ordering temperature and the perpendicular anisotropy strongly depend on the thickness of the Fe film. The magnetic moment of Fe in saturation hardly differs from the bulk value (2.2 μ_B per Fe atom). However, in thin cobalt films on silver, a clear increase of the magnetic moment per Co atom was found – up to 2.15 μ_B , while the bulk value is 1.8 μ_B –. Fig. 6 shows two reflectivity curves for spin parallel and spin parallel for a 1.6-nm-thick Fe film.

REFERENCES

[1] E. Segrè (editor), 'Enrico Fermi, Collected Papers', (University of Chicago Press, Chicago, 1962).
[2] A.G. Klein and S.A. Werner, Rep. Prog. Phys. **46** (1982) 259.
[3] A.G. Klein and S.A. Werner, in Methods of Experimental Physics, Vol. 23 – part A, *Neutron Scattering*, editors K. Sköld and D.L. Price, (Academic Press, Orlando, 1986) Ch. 4.
[4] V.F. Sears, *Neutron Optics*, (Oxford University Press, New York, 1989).
[5] L. Koester and T. Springer, *Neutron Physics*, (Springer Verlag, Berlin, 1977).
[6] H. Mayer-Leibnitz and T. Springer, Reactor Sci. and Techn. Of Nucl. Energy, Parts A and B **17** (1963) 217.
[7] M.Th. Rekveldt, P. Verkerk, and A.A. van Well, Nucl. Instr. Meth. Phys. Res. B **34** (1988) 285.
[8] K. Abrahams, W. Ratynski, F. Stecher-Rasmussen, and E. Warning, Nucl. Instr. Meth. **45** (1966) 293.
[9] F. Mezei, Comm. In Phys. **1** (1976) 81.
[10] M.Th. Rekveldt and W.H. Kraan, Physica B **120** (1983) 81.
[11] S.K. Sinha, E.B. Sirota, S. Garoff, and H.B. Stanley, Phys. Rev. B **38** (1988) 2297.
[12] A. Breslau, P.S. Pershan, G. Swislow, B.M. Ocko, and J. Als-Nielsen, Phys. Rev A **38** (1988) 2457.
[13] J. Lekner, *Theory of Reflection*, (Martinus Nijhoff, Dordrecht, 1987).
[14] G.P. Felcher and T.P. Russel (editors), *Proceedings of the Workshop on Methods of Analysis and Interpretation of Neutron Reflectometry Data*, Physica B **173** Nos. 1&2 (1991).
[15] G.P. Felcher, R.O. Hilleke, R.K. Crawford, J. Haumann, R. Kleb, and G. Ostrowski, Rev. Sci. Instrum. **58** (1987) 609.
[16] S.J. Blundell and J.A.C. Bland, Phys. Rev. B **46** (1992) 3391.
[17] H. Fredrikze and R.W.E. van de Kruijs, to be published.
[18] G.P. Felcher, S. Adenwalla, V.O. de Haan, and A.A. van Well, Nature **377** (1995) 409.
[19] G.P. Felcher, S. Adenwalla, V.O. de Haan, and A.A. van Well, Physica B **221** (1996) 494.
[20] H. Fredrikze, M.Th. Rekveldt, A.A. van Well, Y. Nikitenko, V. Syromyatnikov, Physica B **248** (1998) 157.
[21] H. Kiessig, Ann. Phys. (Leipzig) **10** (1931) 715.
[22] V.O. de Haan, J. de Blois, P. van der Ende, H. Fredrikze, A. van der Graaf, M.N. Schipper, A.A. van Well, and J. van der Zanden, Nucl. Instr. Meth. Phys. Res. A **362** (1995) 434.
[23] J. Penfold and R.K. Thomas, J. Condens. Matter **2** (1990) 1369.
[24] D.S. Sivia, W.A. Hamilton, and G.S. Smith, Physica B **173** (1991) 121.
[25] D.S. Sivia and J.R.P. Webster, Physica B **248** (1998) 327.
[26] V.O. de Haan and G.G. Drijkoningen, Physica B **198** (1994) 24.
[27] V.-O. de Haan, A.A. van Well, S. Adenwalla, and G.P. Felcher, Phys. Rev. B **52** (1995) 10831.
[28] V.-O. de Haan, A.A. van Well, P.E. Sacks, S. Adenwalla, and G.P. Felcher, Physica B **221** (1996) 524.
[29] C.F. Majkrzak, N.F. Berk, Phys. Rev. B **52** (1995) 10825.
[30] C.F. Majkrzak, N.F. Berk, Physica B **248** (1998) 338.
[31] R. Lipperheide, J. Kasper, and H. Leeb, Physica B **248** (1998) 366.
[32] J. Lekner, Physica B **173** (1991) 99.
[33] T.L. Crowley, Physica A **195** (1993) 354.
[34] V.-O. de Haan and A.A. van Well, J. of Neutron Research, **3** (1996) 63.
[35] A.A. van Well, Physica B **180&181** (1992) 959.
[36] J. Penfold *et al.* , J. Chem. Soc. Faraday Trans **93** (1997) 3899.
[37] H. Zabel and I.K. Robinson (Eds.), *SXNS-2, Bad Honef*, Springer-Verlag (Berlin, 1992);
H.J. Lauter and V.V. Pasyuk (Eds.), *SXNS-3, Dubna*, Physica B **198** Nos. 1-3 (1994);
G.P. Felcher and H. You, *SXNS-4, Lake Geneva*, Physica B **221** Nos. 1-4 (1996);
D. Norman and J.R.P. Webster, *SXNS-5, Oxford*, Physica **248** (1998).
[38] E.M. Lee, R.K. Thomas, and R.C. Ward, J. Phys. Chem. **93** (1989) 381.
[39] Y.Y. Huang, C. Liu, and G.P. Felcher, Phys. Rev. B **47** (1993) 183.